4915-13-Q

AD-404 721

RADC-TDR-63-435

4915-13-Q = RL-2116

MICROWAVE PLASMA COMPONENTS STUDY

TECHNICAL DOCUMENTARY REPORT NO. RADC-TDR-63-435
November 1963

Techniques Laboratory
Rome Air Development Center
Research and Technology Division
Air Force Systems Command
Griffiss Air Force Base, New York

Project No. 5573, Task No. 557301

(Prepared under Contract No. AF30(602)-2605 by Andrejs Olte and E.K. Miller, The University of Michigan, Ann Arbor, Michigan)

Suggested Keywords: Magneto-plasma resonance isolator, microwave circuit application

ABSTRACT

First order theory is presented for a magneto-plasma resonance isolator employing the TM_{11} mode in a rectangular waveguide. The effect of non-uniform magnetostatic field on the non-reciprocal transmission properties of the device is investigated. The beginning of experimental study to improve the stability of plasma package in the microwave circuit application is presented.

PUBLICATION REVIEW

This report has been reviewed and is approved. For further technical information on this project, contact Mr. Joseph Schenna, RALTM, Ext. 4251.

Approved: Joseph M. Schenna
JOSEPH SCHENNA
Project Engineer
Directorate of Aerospace Surveillance & Control

Approved: Arthur J. Frohlich
ARTHUR J. FROHLICH
Chief, Techniques Laboratory
Directorate of Aerospace Surveillance & Control

AIR FORCE, Cato Show Prtg. Co. 11/25/63 - 142

TABLE OF CONTENTS

		Page
I.	Theoretical Derivation of Absorption in the Electron Cyclotron Resonance Isolator	1
II.	Experimental Study of Plasma Package Stability	19
III.	Conclusions	22
IV.	Future Plans	23

LIST OF FIGURES

Figure		Page
1-1	Isolator Geometry	2
1-2	Ratio of Power Transmission to P^2 as a Function of Y, Calculated from the Extraordinary Wave Approximation Equation (1.31)	12
1-3	Ratio of Power Transmission to P^2 as a Function of Y, Calculated from the Extraordinary Wave Approximation with Elliptic Polarization Accounted for Equation (1.47)	18
2-1	Vacuum System	20

INTRODUCTION

This Quarterly Progress Reports presents work done on Air Force Contract AF 30(602)-2605 for the period 1 April to 30 June 1963.[+] This report has three sections. Section I presents partially completed theoretical work on the mode of absorption of the electron cyclotron resonance isolator. Section II gives an account of the progress made in the experimental phase of the effort. Section III presents a brief statement of the plans for the second quarter. Previous work on these problems is summarized in Radiation Laboratory Report 4915-1-F(RADC-TDR-63-54).

I. THEORETICAL DERIVATION OF ABSORPTION IN THE ELECTRON CYCLOTRON RESONANCE ISOLATOR.

We want to compute the power transmission coefficient through a plasma cyclotron resonance isolator. The pertinent dimensions of the isolator and the coordinate systems are shown in Fig. I-1. A TM_{11} mode propagates in the square cross section waveguide in the positive z-direction. A thin plasma slab in the bottom half of the waveguide extends from wall to wall in the x-direction. A magnetostatic field is impressed on the plasma in the +x-direction.

The power flow at each point in the z-direction, for any waveguide, may be characterized by an absorption coefficient α that is defined by

[+]Note: Although this is called Quarterly Status Report No. 13 it should be noted that it covers work done in the first quarter of the second year. The first 12 reports were monthly.

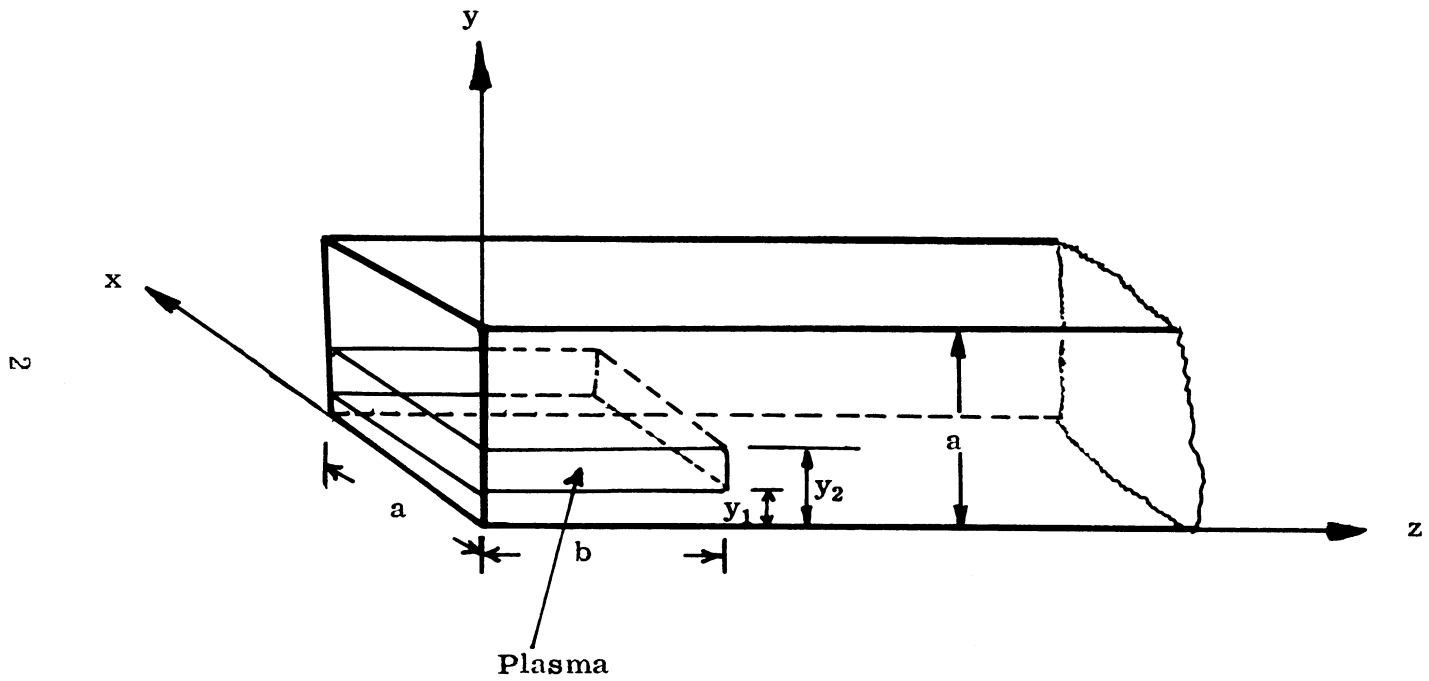

FIGURE I-1.

a = 7.6cm, b = 7.7cm, y_1 = 1.0cm, and y_2 = 2.5 cm.

(assuming propagation in the positive z-direction)

$$P(z) = P_{in}\exp\left[-2\int^{z}\alpha(z')dz'\right] \tag{1.1}$$

where P_{in} is the input power, and P(z) is the remaining power as the wave progresses through the guide. Differentation of (1.1) yields ,

$$\alpha(z) = -\frac{1}{2P(z)}\frac{dP(z)}{dz} \tag{1.2}$$

But since the time average of the divergence of the Poyntings vector, $\overline{\nabla \cdot \bar{S}}$, gives the negative density of the power absorbed in the medium we obtain,

$$\frac{dP(z)}{dz} = \iint_{A}\overline{\nabla \cdot \bar{S}}\,dx\,dy \quad , \tag{1.3}$$

where A is the guide cross section. On substituting (1.3) in (1.2) we have

$$\alpha(z) = -\frac{1}{2P(z)}\iint_{A}\overline{\nabla \cdot \bar{S}}\,dx\,dy \quad . \tag{1.4}$$

The power transmission coefficient (PTC) of the isolator may now be defined by

$$PTC \equiv 10\log\frac{P_{out}}{P_{in}} \tag{1.5}$$

Neglecting the reflections from the ends of the isolator we have

$$PTC = 4.34 \int_0^b \alpha(z')dz' \tag{1.6}$$

and since

$$P(z) = \frac{1}{2} \mathrm{Re} \iint_A \bar{S} \cdot \bar{a}_z \, dx \, dy \tag{1.7}$$

we have from (1.4) and (1.6) that

$$PTC = 4.34 \int_0^b \left\{ \frac{\iint_A \overline{\nabla \cdot \bar{S}} \, dx \, dy}{\mathrm{Re} \iint \bar{S} \cdot \bar{a}_z \, dx \, dy} \right\} dz \tag{1.8}$$

We see that in order to calculate the PTC one must have a model that describes the plasma-electromagnetic wave interaction so that the divergence of the power flow may be obtained.

The magneto-ionic plasma has a permittivity of the following form in our coordinate system:

$$\epsilon = \begin{bmatrix} \epsilon_{11} & 0 & 0 \\ 0 & \epsilon_{22} & \epsilon_{23} \\ 0 & \epsilon_{32} & \epsilon_{33} \end{bmatrix} \tag{1.9}$$

The tensor elements are given by

$$\epsilon_{11} = \epsilon_0 \left[1 + \frac{P^2}{j(V+j)} \right]$$

$$\epsilon_{22} = \epsilon_{33} = \epsilon_0 \left[1 + \frac{P^2(V+j)}{j\,(V+j)^2 + Y^2} \right] \tag{1.10}$$

$$\epsilon_{23} = -\epsilon_{32} = \epsilon_0 \left[\frac{j\,Y\,P^2}{(V+j)^2 + Y^2} \right]$$

where $P = \omega_P/\omega$, $V = \nu_c/\omega$, $Y = \omega_H/\omega$.

The time average divergence of Poyntings vector for an anisotropic dielectric is given by

$$\overline{\nabla \cdot \bar{S}} = -j\frac{\omega}{4}\left[\epsilon_{ik} - \epsilon^*_{ki}\right] \; E_i \, E^*_k \tag{1.11}$$

In the above formula the tensor notation is used. Substituting (1.9) and (1.10) in (1.11) we have

$$\overline{\nabla \cdot \bar{S}} = -j\frac{\omega}{4}\Big\{(\epsilon_{11}-\epsilon^*_{11})E^*_1 E_1 + (\epsilon_{22}-\epsilon^*_{22})(E^*_2 E_2 + E^*_3 E_3) + (\epsilon_{23}+\epsilon^*_{23})(E^*_2 E_3 - E^*_3 E_2)\Big\} \tag{1.12a}$$

with

$$\epsilon_{11} - \epsilon^*_{11} = -2j\,\epsilon_0 \frac{VP^2}{1+V^2} \tag{1.12b}$$

$$\epsilon_{22} - \epsilon^*_{22} = -2j\,\epsilon_0 \frac{VP^2(Y^2+V^2+1)}{(Y^2+V^2-1)^2+(2V)^2} \tag{1.12c}$$

$$\epsilon_{23} + \epsilon^*_{23} = 4\,\epsilon_0 \frac{VP^2\,Y}{(Y^2+V^2-1)^2+(2V)^2} \tag{1.12d}$$

The isolator is operated normally a state such that the following conditions on the parameters hold true:

$$V \ll 1 \tag{1.13a}$$

and

$$Y = 1+\Delta Y \quad , \qquad |\Delta Y| \ll 1 \, . \tag{1.13b}$$

The conditions (1.13 a and b) imply that the first term on the right hand side of (1.12a) is negligible compared to the remaining two terms. Thus further we consider only that

$$\overline{\nabla \cdot \bar{S}} \cong -j \frac{\omega}{4} \left\{ (\epsilon_{22} - \epsilon_{22}^*)(E_2^* E_2 + E_3^* E_3) + (\epsilon_{23} + \epsilon_{23}^*)(E_2^* E_3 - E_3^* E_2) \right\} \tag{1.14}$$

A special case of considerable interest is when the electrical field part containing E_2 and E_3 components is circularly polarized. Then

$$E_3 = \mp j E_2 \tag{1.15}$$

and

$$\overline{\nabla \cdot \bar{S}} \simeq -\epsilon_0 \frac{\omega}{2} V P^2 \frac{(Y \mp 1)^2 + V^2}{(V^2+Y^2-1)^2 + (2V)^2} |E|^2 \tag{1.16}$$

where

$$|E|^2 = 2 |E_2|^2 = 2 |E_3|^2$$

and the $\mp$ signs are correlated with the signs in (1.15). Applying conditions (1.13) to (1.16) and taking the leading terms we have in the case of the (-) sign

$$\overline{\nabla \cdot \bar{S}_{(-)}} \simeq -\epsilon_0 \frac{\omega}{2} VP^2 \frac{1}{4} |E|^2 \tag{1.17}$$

and in case of the (+) sign

$$\overline{\nabla \cdot \bar{S}_{(+)}} \simeq -\epsilon_0 \frac{\omega}{2} VP^2 \frac{1}{(\nabla Y)^2 + V^2} |E|^2 \tag{1.18}$$

Equations (1.17) and (1.18) show that the time average divergence in the vicinity of the cyclotron resonance very strongly depends on the sense of the circular polarization of the electric field in the plane normal to the magnetostatic field. This is due to the fact that the sense of rotation of the electrons in a plane normal to the magnetostatic field is fixed, and in the case of (1.18) the electric field is rotating in the same sense whereas in (1.17) the electric field is rotating in the opposite sense to the natural direction of the electron rotation. Hence we have the striking difference in the time average of the Poyntings vector divergence.

For the moment we leave this thread of reasoning and consider the following. The time average divergence of the Poyntings vector in an isotropic medium that has only dielectrical losses may be written as

$$\overline{\nabla \cdot \bar{S}} = -\frac{\omega}{2} \epsilon'' \bar{E} \cdot \bar{E}^* \tag{1.19}$$

where $\epsilon = \epsilon' - j\epsilon''$ is the permittivity of the medium and clearly is a scalar constant. However, also in the special case of a circularly polarized plane

wave that is propagating along the magnetostatic field line the electrical flux density is related to the electrical field by a scalar constant; an equivalent permittivity so to speak. We distinguish two waves: ordinary and extra-ordinary, depending on the sense of polarization of the electrical field. For the extraordinary wave the sense of polarization of the electrical field is the same as the direction of rotation of electrons in the magnetostatic field, while for the ordinary wave they are opposite. One may be tempted to believe that it is permissible to take the imaginary parts of these equivalent permittivities and substitute them in (1.19). Then we obtain that in the case of extraordinary wave

$$\overline{\nabla \cdot \bar{S}}_{ex.} = -\epsilon_0 \frac{\omega}{2} VP^2 \frac{1}{(Y-1)^2+V^2} \bar{E} \cdot \bar{E}^* \quad , \tag{1.20}$$

and in the case of ordinary wave

$$\overline{\nabla \cdot \bar{S}}_{ord.} = -\epsilon_0 \frac{\omega}{2} VP^2 \frac{1}{(Y+1)^2+V^2} \bar{E} \cdot \bar{E}^* \tag{1.21}$$

The absorption for the ordinary wave should correspond to (1.16) with the (-) sign while the same equation with the (+) sign would apply to the absorption of the extraordinary wave. Equation (1.16), however, does not reduce any further, and we have to conclude that (1.20) and (1.21) in general are not correct. But here, we are not interested in the total domain of the variables. We are interested primarily in conditions (1.13). When we apply conditions (1.13) to (1.20) and (1.21) we have respectively:

$$\overline{\nabla \cdot \bar{S}}_{ex.} \simeq -\epsilon_0 \frac{\omega}{2} VP^2 \frac{1}{(\nabla Y)^2+V^2} \bar{E} \cdot \bar{E}^* \tag{1.22}$$

and

$$\overline{\nabla \cdot \bar{S}}_{ord.} = -\epsilon_0 \frac{\omega}{2} VP^2 \frac{1}{4} \bar{E} \cdot \bar{E}^* \tag{1.23}$$

It is clear that (1.22) corresponds to (1.18) and (1.23) corresponds to (1.17). We may conclude that (1.20) and (1.21) are a good approximation to the actual absorption in the magneto-ionic medium in the case when the microwave frequency is close to the electron cyclotron frequency and the electron collision frequency is small compared to the first. With these approximations in mind we will be using (1.20) and (1.21) in the first set of calculations. To shorten the notation we introduce the following.

$$\epsilon''_+ = \epsilon_0 VP^2 \frac{1}{(Y-1)^2+V^2} \tag{1.24}$$

and

$$\epsilon''_- = \epsilon_0 VP^2 \frac{1}{(Y+1)^2+V^2} \tag{1.25}$$

Before we can proceed with the calculation of the power transmission coefficient we have to write down the form of the fields in the isolator. We consider the fields of the TM_{11} mode propagating in the positive z-direction in an empty guide. Within an arbitrary constant and assuming $e^{j\omega t}$ time dependence, they are

$$\bar{E} = \left[-j\beta_{11} a \cos\frac{\pi x}{a} \sin\frac{\pi y}{a}\, \bar{a}_x - j\beta_{11}\, a \sin\frac{\pi x}{a} \cos\frac{\pi y}{a}\, \bar{a}_y \right.$$

$$\left. + 2\pi \sin\frac{\pi x}{a} \sin\frac{\pi y}{a}\, \bar{a}_z \right] e^{-j\beta_{11} z} \qquad (1.26)$$

$$\bar{H} = j\omega\, \epsilon_0 a \left[\sin\frac{\pi x}{a} \cos\frac{\pi y}{a}\, \bar{a}_x - \cos\frac{\pi x}{a} \sin\frac{\pi y}{a}\, \bar{a}_y \right] e^{-j\beta_{11} z} \qquad (1.27)$$

where

$$\beta_{11} = \sqrt{\omega^2 \mu_o \epsilon_o - 2\left(\frac{\pi}{a}\right)^2} \quad .$$

In the context of using formulas (1.20) and (1.21) we neglect E_x and hence we have

$$\bar{E} \cdot \bar{E}^* = a^2 \beta_{11}^2 \cos^2\frac{\pi y}{a} \sin^2\frac{\pi x}{a} + 4\pi^2 \sin^2\frac{\pi x}{a} \sin^2\frac{\pi y}{a} \qquad (1.28)$$

Furthermore we have that

$$\int_A \int \overline{\bar{S} \cdot \bar{a}_z}\, dxdy = \frac{1}{2} \mathrm{Re} \iint_A \bar{E} \times \bar{H}^* \cdot \bar{a}_z\, dxdy = \frac{1}{4} \omega \epsilon_o \beta_{11} a^4 \qquad (1.29)$$

We observe that (1.24) has to be used together with the fields of (1.26). Thus we have

$$\overline{\nabla \cdot \bar{S}} = -\frac{\omega}{2} \epsilon'' \left[a^2 \beta_{11}^2 \sin^2\frac{\pi x}{a} \cos^2\frac{\pi y}{a} + 4\pi^2 \sin^2\frac{\pi x}{a} \sin^2\frac{\pi y}{a} \right] \qquad (1.30)$$

Substituting (1.29) and (1.30) in (1 8) we have

$$PTC = -8.68 \int_0^b dz \int_{y_1}^{y_2} dy \int_0^a dx \left[\frac{\beta_{11}}{a^2} \sin^2 \frac{\pi x}{a} \cos^2 \frac{\pi y}{a} + \frac{4\pi^2}{\beta_{11} a^4} \sin^2 \frac{\pi x}{a} \sin^2 \frac{\pi y}{a} \right] \frac{\epsilon''_+}{\epsilon_0} \qquad (1.31)$$

When ϵ''_+ in the preceding equation is independent of coordinates, we may easily carry out the integration, and

$$PTC = \frac{109b}{\beta_{11} a^2} \left[0.173 \left(\frac{\beta_{11} a}{2\pi} \right)^2 + 0.136 \right] \frac{\epsilon''_+}{\epsilon_0} \qquad (1.32)$$

For a frequency of 3.9 Gc the equation (1.32) reduces to

$$PTC = -5.6 \frac{P^2 V}{(Y-1)^2 + V^2} \qquad (1.33)$$

In Fig. I-2 the ratio PTC to P^2 of (1.33) is plotted as a function of Y for f = 3.9 Gc and ν_c = 0.8 Gc. The magnetostatic field strength is taken at the center of the plasma. We observe a sharp resonance at Y=1, i.e. $\omega = \omega_H$.

Measurements on the magnetostatic field show that the field at the center of the plasma chamber is about 15 percent less than that at the edges. Since ϵ''_+ is dependent upon the cyclotron frequency and hence on the magnetostatic field strength, it follows that (1.32) is not strictly applicable in our case.

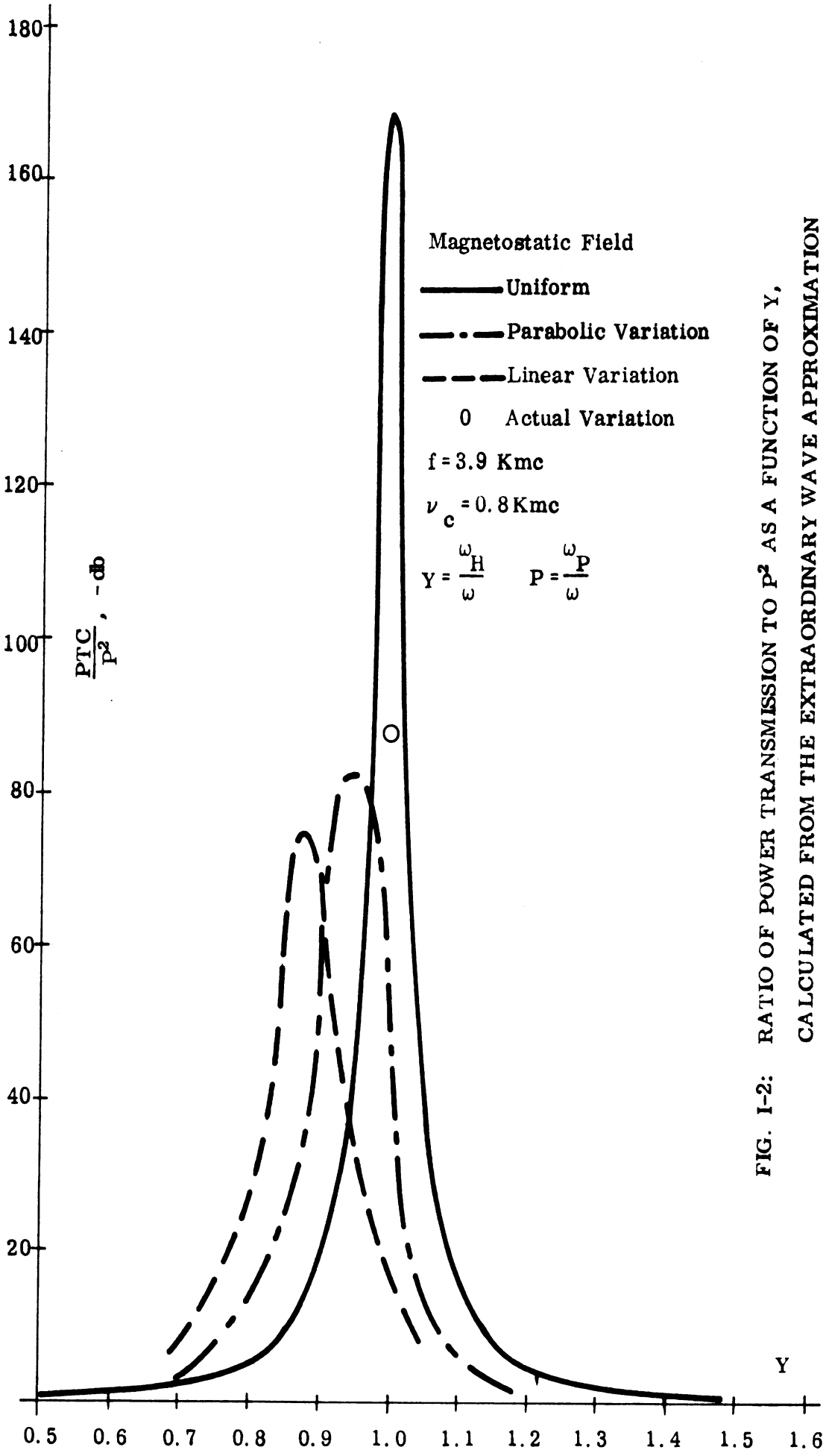

FIG. I-2: RATIO OF POWER TRANSMISSION TO P^2 AS A FUNCTION OF Y, CALCULATED FROM THE EXTRAORDINARY WAVE APPROXIMATION [EQUATION (1.31)]

In order to determine the effect upon the PTC of a non-uniform magnetostatic field, the integration of (1.31) was performed assuming a parabolic and a linear variation of the magnetostatic field in the x- and z-directions. Since the extent of the plasma in the y-direction is rather small compared to the waveguide size, the magnetostatic field in this coordinate was assumed constant. The integration was performed numerically, using, as before, a microwave frequency of 3.9 Gc and a collision frequency of 0.8 Gc. In Fig. I-2 we have shown the PTC to P^2 ratios for the parabolic and linear field variation. We notice that the resonance absorption peaks are considerably broadened, and reduced in amplitude by approximately one-half as compared to the constant magnetostatic field case. For Y=1 the PTC/P^2 was computed for the measured magnetostatic field variation. It is slightly larger than the preceding two magnetic field variation cases.

At this point we should summarize the approximations which have not been pointed out explicitly in the calculation of the graphs of Fig. I-2.

(1) The field in the plasma has the same transverse variation as in the empty guide and there is no reflected wave in the plasma section of the guide. This assumption will also be used in subsequent calculations.

(2) The longitudinal electric field of the TM_{11} mode is not circularly polarized throughout the plasma cross section, but we are proceeding as if it were.

(3) The magneto-ionic plasma slab does not convert energy from the TM_{11} mode into the TE_{10} or TE_{01} mode which are also propagating modes in our square waveguide.

When the direction of propagation of the TM_{11} mode is reversed, i.e. it is propagating in the negative z-direction, then the PTC may be computed from (1.31) by substituting for ϵ''_- the imaginary part of the equivalent permittivity for the ordinary wave, ϵ''_+, given by (1.25). This loss is negligible for $V \ll 1$ and $Y \sim 1$; our region of interest.

In the preceding discussion it was assumed that the longitudinal field of the TM_{11} mode was circularly polarized throughout the plasma slab. The assumption holds only for the center plane of the slab. In the rest of it the field is elliptically polarized. We may remove this approximation, if we decompose the elliptically polarized electric field into two oppositely rotating, unequal amplitude, circularly polarized fields. We thus let

$$\bar{E} = \left[\bar{A}_+ + \bar{B}_- \right] e^{-j\beta_{11} z} \tag{1.34}$$

with

$$\bar{A}_+ = A_2 \bar{a}_y + jA_3 \bar{a}_z \tag{1.35a}$$

$$\bar{B}_- = B_2 \bar{a}_y - jB_3 \bar{a}_z \tag{1.35b}$$

and

$$A_2 = A_3, \qquad B_2 = B_3 \quad .$$

The longitudinal electric field then is resolved as

$$A_2 = -\frac{1}{2} j \sin\frac{\pi x}{a}\left[a\beta_{11}\cos\frac{\pi y}{a} + 2\pi \sin\frac{\pi y}{a}\right] \tag{1.36a}$$

$$B_2 = -\frac{1}{2} j \sin\frac{\pi x}{a}\left[a\beta_{11}\cos\frac{\pi y}{a} - 2\pi \sin\frac{\pi y}{a}\right] \tag{1.36b}$$

We notice that for our range of parameters $B_2 \ll A_2$. The time average divergence of the Poyntings vector becomes

$$\nabla \cdot \bar{S} \cong -\frac{\omega}{2}\left[\epsilon''_+ \bar{A}_+ \cdot \bar{A}^*_+ + \epsilon''_- \bar{B}_- \cdot \bar{B}^*_-\right] \tag{1.37}$$

It would appear that we are mis-using superposition to obtain the above formula. In fact we are not using that principle in either sense. We may easily show that the power absorption in the magneto-ionic medium does not couple for the ordinary and the extraordinary waves. We consider a medium that has only dielectric losses. Then

$$\overline{\nabla \cdot \bar{S}} = -\overline{\bar{E} \cdot \frac{\partial \bar{D}}{\partial t}} \tag{1.38}$$

Considering two circularly polarized waves:

$$\bar{D}_1 = \epsilon_1 \bar{E}_1 \; ; \quad \epsilon_1 = \epsilon'_1 - j\epsilon''_1 \tag{1.39a}$$

and

$$\bar{D}_2 = \epsilon_2 \bar{E}_2 \; ; \quad \epsilon_2 = \epsilon'_2 - j\epsilon''_2 \tag{1.39b}$$

with

$$\bar{E}_1 = E_1 (\bar{a}_x + j\bar{a}_y) \tag{1.40a}$$

$$\bar{E}_2 = E_2(\bar{a}_x - j\bar{a}_y) \tag{1.40b}$$

We introduce complex notation in (1.38) by letting

$$\bar{E} \longrightarrow \frac{1}{2}(\bar{E}_1 + \bar{E}_1^*) + \frac{1}{2}(\bar{E}_2 + \bar{E}_2^*) \tag{1.41}$$

$$\frac{\partial \bar{D}}{\partial t} \longrightarrow \frac{1}{2}(j\omega\epsilon_1 - j\omega\epsilon_1^* E_1^*) + \frac{1}{2}(j\omega\epsilon_2 \bar{E}_2 - j\omega\epsilon_2^* E_2^*) \tag{1.42}$$

and substituting the two preceding equations in (1.38) we obtain

$$\overline{\nabla \cdot \bar{S}} = -\frac{\omega}{2}\left[\epsilon_1'' \bar{E}_1 \cdot \bar{E}_1^* + \epsilon_2'' \bar{E}_2 \cdot \bar{E}_2^*\right] - \frac{\omega}{2}\left[(\epsilon_2 - \epsilon_1^*)\bar{E}_1^* \cdot \bar{E}_2 + (\epsilon_1 - \epsilon_2^*)\bar{E}_1 \cdot \bar{E}_2^*\right] \tag{1.43}$$

Applying (1.40a) and (1.40b) in (1.43) we see that

$$\bar{E}_1^* \cdot \bar{E}_2 = E_1^* E_2 (\bar{a}_x - j\bar{a}_y) \cdot (\bar{a}_x + j\bar{a}_y) = 0 \tag{1.44}$$

$$\bar{E}_1 \cdot \bar{E}_2^* = E_1 E_2^* (\bar{a}_x + j\bar{a}_y) \cdot (\bar{a}_x + j\bar{a}_y) = 0 \tag{1.45}$$

and hence the second term vanishes in (1.43) and consequently we have established that (1.37) is valid, subject only to approximations discussed previously.

We return to the calculation of the power transmission coefficient. In (1.37) we may neglect the second term. Substituting the remainder in (1.8) in the same sense as before we obtain:

$$PTC = -4.34 \int_0^b dz \int_{y_1}^{y_2} dy \int_0^a dx \left\{ \frac{\epsilon''_+}{\epsilon_0} \sin^2 \frac{\pi x}{a} \left[\frac{4\pi^2}{\beta_{11} a^4} \sin^2 \frac{\pi y}{a} + \frac{\beta_{11}}{a^2} \cos^2 \frac{\pi y}{a} + \right. \right.$$

$$\left. \left. + \frac{4\pi}{a^3} \sin \frac{\pi y}{a} \cos \frac{\pi y}{a} \right] \right\} \qquad (1.46)$$

For constant magnetostatic field we can integrate the above equation to

$$PTC = \frac{-54.5b}{\beta_{11} a^2} \frac{\epsilon''_+}{\epsilon_0} \left[0.136 + 0.197 \frac{\beta_{11} a}{2\pi} + 0.173 \left(\frac{\beta_{11} a}{2\pi} \right)^2 \right] \qquad (1.47)$$

We have calculated the ratio of PTC to P^2 for f = 3.9 Gc and ν_c = 0.8 Gc. The results are plotted in Fig. I-3. Comparing this with the corresponding curve in Fig. I-2, we notice that in this particular case the absorption is about 20 percent less on the db scale than it was for the circularly polarized case.

FIG. I-3: RATIO OF POWER TRANSMISSION TO P^2 AS FUNCTION OF Y, CALCULATED FROM THE EXTRAORDINARY WAVE APPROXIMATION WITH ELLIPTIC POLARIZATION ACCOUNTED FOR [EQUATION (1.47)] f = 3.9 Gc, ν_c = 0.8 Gc, $Y = \omega_H / \omega$, $P = \omega_p / \omega$.

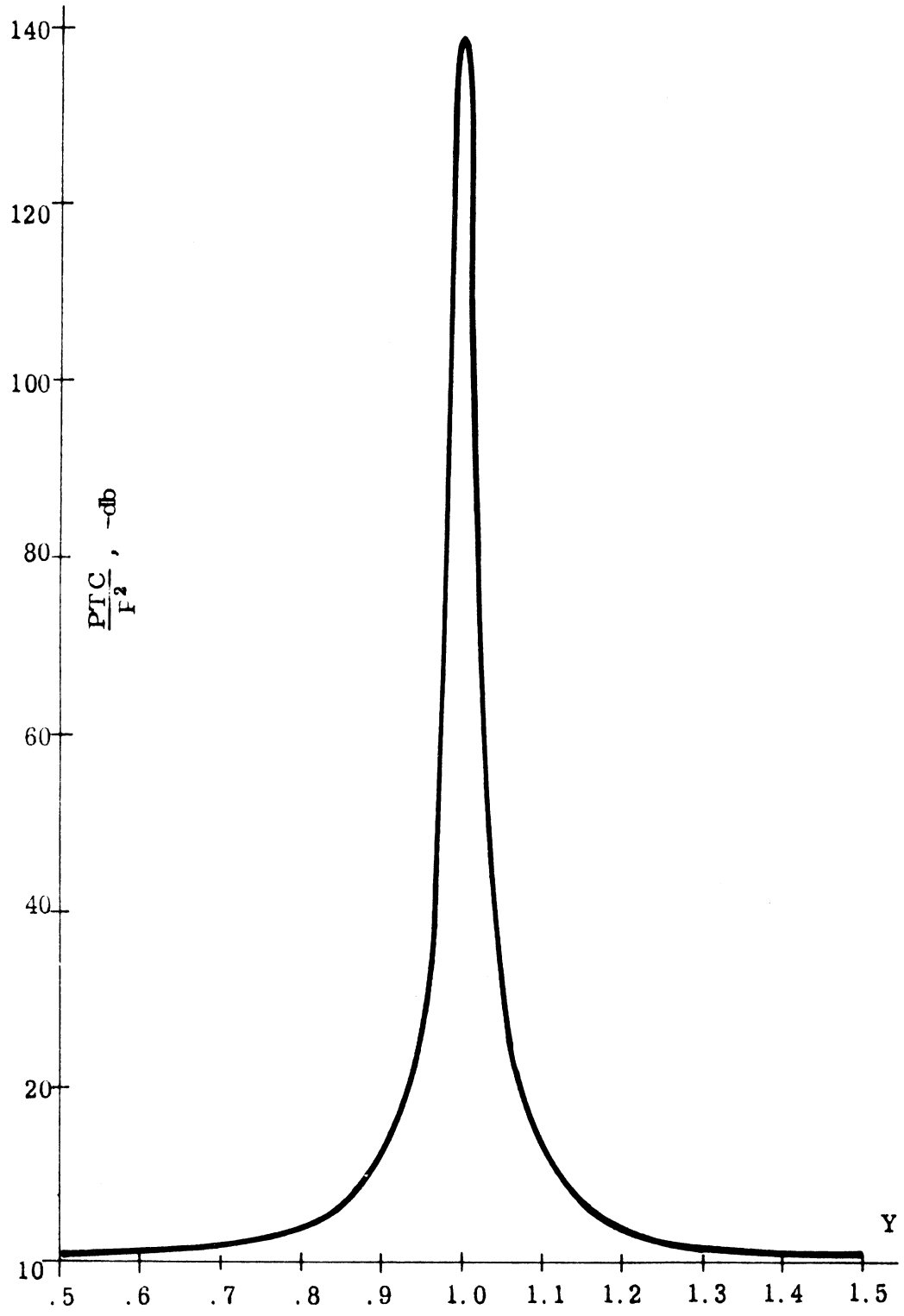

II. EXPERIMENTAL STUDY OF PLASMA PACKAGE STABILITY

2.1 VACUUM SYSTEM

A Varian designed vacuum system employing a 140 liter/sec ion pump was used to evacuate the glass envelope which serves as the plasma chamber. The vacuum system is connected to a glass manifold through a 1 in. copper line. A pressure gauge sensing element, gas inlet port and taper to which the plasma envelope is connected form a part of the glass manifold. A diagram of the vacuum system is shown in Fig. 2-1.

A mechanical forepump is used to take the glass manifold and copper line from atmosphere to about 20 microns Hg. The valve to the Varian system is then opened. A pressure of about 10^{-5} mm Hg was attained at the taper to which the plasma envelope is connected with the Varian system valve fully opened. The ion pump pressure under these conditions is less than 5×10^{-7} mm Hg.

2.2 PLASMA TUBE

A glass envelope 6 cm x 7 cm x 1.5 cm was blown of Pyrex glass. A cathode consisting of 4 straight pieces of thoriated tungsten wires 0.010 in. in diameter welded at the ends to 0.10 in. diameter tungsten rod which served as feed-throughs was placed across the 6 cm end. An anode, also of 0.10 in. diameter tungsten rod, was put across the other end of the envelope. The pumping outlet was located on the anode end of the chamber.

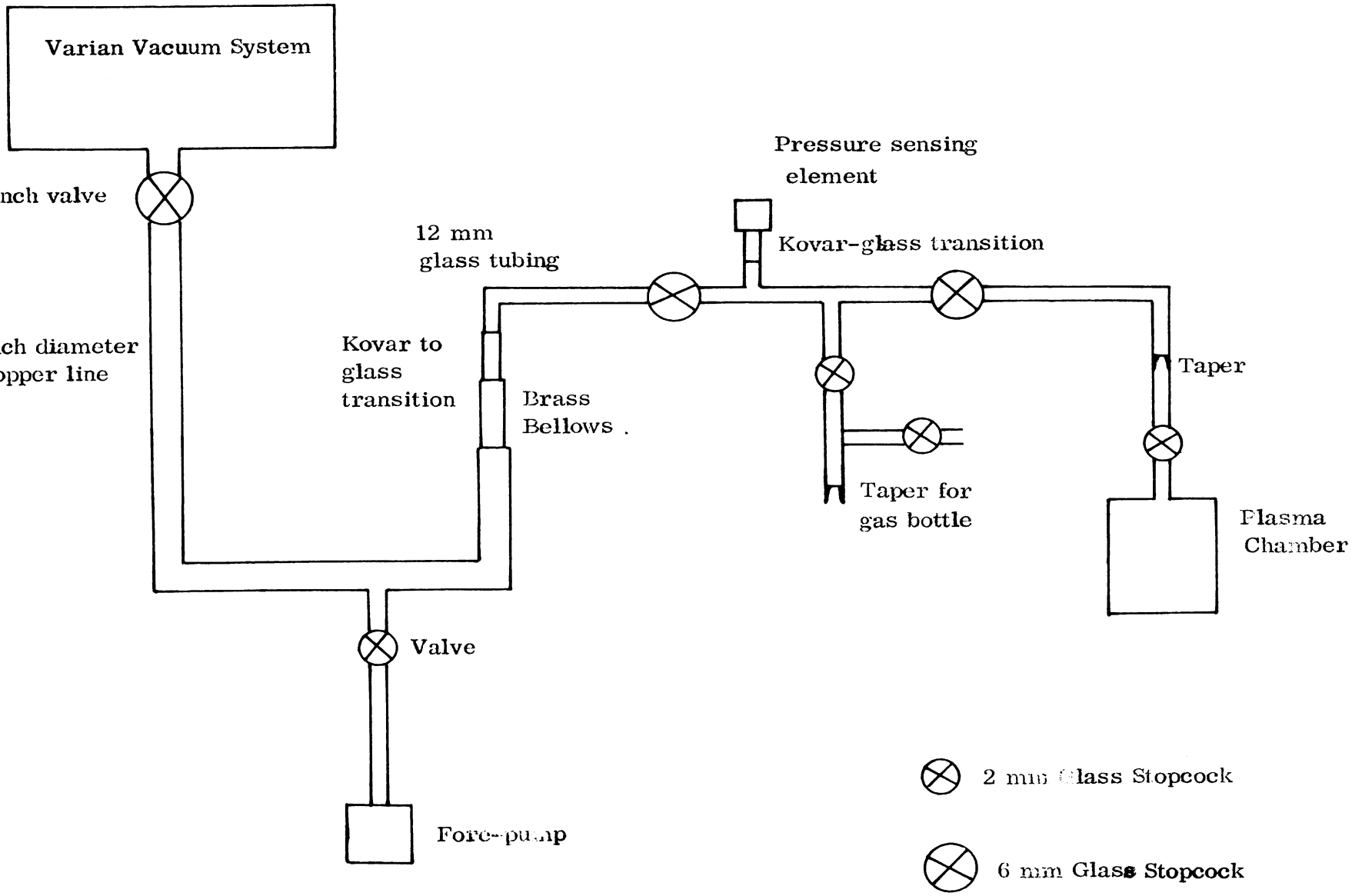

FIGURE 2-1: VACUUM SYSTEM

The cathode design was tested by inserting a second cathode in a glass envelope and heating the cathode to temperatures as high as $3000^{o}K$ after evacuation of the envelope. The welds held satisfactorily at these temperatures, which are much higher than the normal operating temperatures of 1800 to $1900^{o}K$. The temperature limited emission of the cathode was calculated to be about 1 ampere at $1900^{o}K$.

2.3 CATHODE DEVELOPMENT

A small oven was constructed of toaster heater elements for baking the plasma envelope. Temperatures as high as $550^{o}C$ could be attained and were varied by means of a variac.

The envelope was baked at $350^{o}C$ for 2 days, while either on the Varian system or being evacuated by the mechanical fore pump. The initial attempt to bake out the chamber revealed the presence of an intermittant leak through two of the feed-throughs. After reworking of the chamber, the chamber was evacuated, and while it was being baked, the Varian system remained at a pressure less than 5×10^{-7} mm Hg with the valve fully open, with no indication of a leak.

Cathode temperature measurements were made by use of an optical pyrometer and measurements of the cathode resistance. The resistance has been used previously as a temperature indication and has been found to correlate quite well with the optical pyrometer.

The cathode activation was begun by heating the cathode to about 1000^{o}K while baking out the chamber. When the outgasing had ceased, the cathode temperature was further increased to 1800^{o}K. The activation was continued by flashing the cathode to temperatures between 2200 to 2500^{o}K for periods up to 30 seconds and then returning to 1800^{o}K. A voltage was then applied between the cathode and anode to determine if there was a measureable emission. In this manner, the cathode emission was gradually increased to 3 ma at an anode potential of 200 V.

Shortly after, the emission began to decrease, and eventually fell to about 4 μa at 200 V. Efforts to return the emission to its former value proved fruitless. We concluded that the decreased emission was most likely the result of either (1) poisoning of the cathode by gas sputtered from the anode or (2) evaporation of all the free thorium from the cathode. In order to remedy this situation, future anodes will be baked out separately at higher temperatures and we will attempt to use lower activation temperatures.

III. CONCLUSIONS

The theoretical work provides tractable formulas to predict the optimum performance of the magneto-ionic resonance isolator. The implications of these formulas need to be studied and compared with existing data from the experimental model of the device.

IV FUTURE PLANS

In the next quarter, attention will be directed towards the cathode development. A helical design will be tried, as well as the possibility of obtaining a suitable commercially manufactured cathode. With a successfully developed cathode, the plasma envelope will be placed in an rf cavity, and the plasma frequency and collision frequency investigated as a function of gas type and pressure. Reproducibility of the results will be emphasized in this work. This data will be used to find the optimum gas parameters to be used in a sealed plasma envelope for electron cyclotron resonance interaction.